2 January 1998

ELSEVIER

Chemical Physics Letters 282 (1998) 7–15

CHEMICAL PHYSICS LETTERS

Electronic interaction and charge transfer efficiencies in triaromatic donor–acceptor systems. An experimental and theoretical study

T. Fiebig *, W. Kühnle, H. Staerk

Max-Planck-Institut für biophysikalische Chemie, Abteilung Spektroskopie und photochemische Kinetik, Am Fassberg, D-37077 Göttingen, Germany

Received 28 July 1997; in final form 8 October 1997

Abstract

To address the issue of electronic interaction between donor (D) and acceptor (A) moieties in intramolecular charge transfer reactions a series of chemically closely related extended π-systems has been investigated. These compounds contain pyrene and organic methyl ester derivatives connected via a phenyl group. Our steady-state fluorescence studies reveal that only particular compounds exhibit strong charge transfer (CT) emission in solution. To elucidate the experimental results we have performed semiempirical CNDO/S-CI calculations which indicate that the electronic coupling and Coulomb stabilization of the CT state are strongly dependent on the nodal properties of the D/A orbitals. © 1998 Elsevier Science B.V.

1. Introduction

Intramolecular charge transfer (CT) reactions in conjugated organic systems have been widely investigated during the last decades following the goal to understand the factors that control the efficiencies of charge separation and charge recombination [1–10]. In this Letter we want to focus on the influence of structural factors on overall charge transfer efficiencies in donor (D)–acceptor (A) substituted extended π-systems.

According to widely accepted theories the charge transfer dynamics are influenced by a *nuclear* factor — the Franck–Condon weighted density of states (FCWD) — and an *electronic* factor which is related to the electronic coupling matrix element H [11–13]. The FCWD depends — among other factors — strongly on the reactions' free enthalpy ΔG°, i.e. on the redox properties of donor and acceptor [14]. It is common practice to apply the electrochemical redox potentials which have been obtained for donor and acceptor *separately* — even when both moieties are covalently linked.

However, one issue of this Letter is to address the problem of using those data for intramolecular CT processes. To focus on effects that are primarily due to differences in the electronic structure of the molecular system one has to develop compounds which show significant differences in the spatial properties of their relevant wavefunctions for CT.

* Corresponding author. Present address: Arthur Amos Noyes Laboratory of Chemical Physics, California Institute of Technology, Pasadena, CA 91125, USA. E-mail: tfiebig@cco.caltech.edu

PII S0009-2614(97)01161-5

However, these systems should also be chemically closely related to each other to avoid strong differences in other parameters contributing to the FCWD in the rate equation.

One way to realize this goal — as good as possible — is to keep donor and acceptor moieties constant within a series of compounds and to carry out appropriate changes in the substitution scheme and the linkage positions between D and A, respectively.

For this purpose we have synthesized several bichromophoric systems containing phthalic acid ester, isophthalic acid ester and benzoic acid ester (as electron acceptors) linked to pyrene (electron donor,

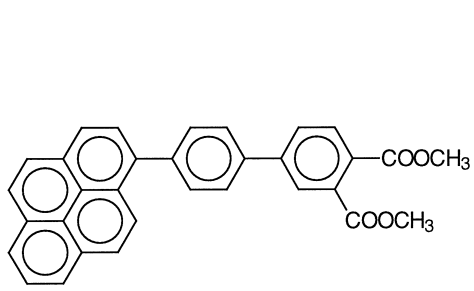

1e34

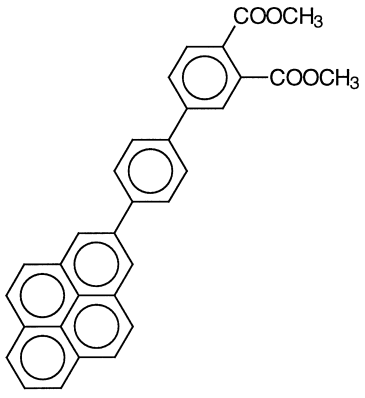

2e34

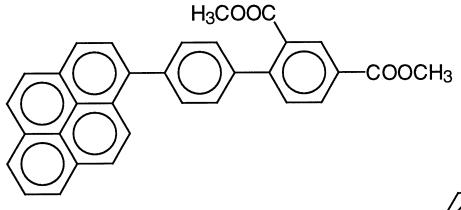

1e24

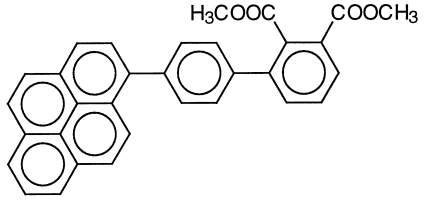

1e23

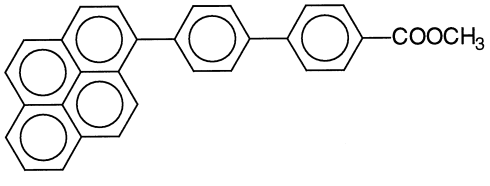

1e4

Scheme 1.

after excitation) via a phenyl group (see Scheme 1). Details about the preparation will be described elsewhere.

Here, we give a first report about their fluorescence and absorption properties in solution. Moreover, we try to elucidate the huge differences in the stationary spectra on the basis of quantum chemical calculations using the semiempirical CNDO/S method [15,16]. We discuss the photophysical mechanism of CT formation in terms of a three-level system: the excitation from the electronic ground state leads to an electronically excited state which is assumed to be predominantly localized on the pyrene site (LE). The latter can either relax to the electronic ground state (radiatively or nonradiatively) or undergo CT formation.

2. Methodology

2.1. Experimental

All compounds have been purified by HPLC. The samples have been degassed by 8–10 freeze/pump/thaw cycles. Solvents were obtained from Merck (UVASOL, spectroscopic grade). All stationary fluorescence spectra were obtained with a Perkin Elmer LS50 fluorimeter. The spectra were intensity corrected using a reference spectrum of a calibrated tungsten halogen lamp. The absorption spectra were recorded with a Varian Cary 5e spectrometer. Fluorescence lifetimes were measured using a time-correlated single-photon-counting apparatus (Edinburgh Instruments).

2.2. Computational: geometry optimization

The equilibrium conformations of all compounds in their electronic ground states have been determined by semiempirical AM1 calculations using the MOPAC 6.0 Package [17].

2.3. Computational: spectroscopic properties

The excitation energies and oscillator strengths for simulating the ground state absorption spectra and excited state properties have been calculated using the CNDO/S-CI method [15,16]. Configuration interaction (CI) with 200 singly excited configurations has been taken into account.

All calculated properties are referred to free molecules in the gas phase since no solvation contributions are included in the Hamiltonian. The calculations have been executed on IBM/RS6000 POWER2 Workstations as well as on a 200 MHz Pentium PC.

3. Results

3.1. 1- and 2-pyrene derivatives

3.1.1. Experimental

Fig. 1a shows the fluorescence spectra of **1e34** and **2e34** in acetonitrile. For **2e34** one can observe a weakly structured band with a maximum at ~405 nm. This spectrum can clearly be attributed mainly to LE-type fluorescence of the pyrene moiety. The appearance of this band can be ascribed to a relatively low CT efficiency in this system, i.e. the charge separation is slow compared to the decay channels of the CT state, which are reformation of

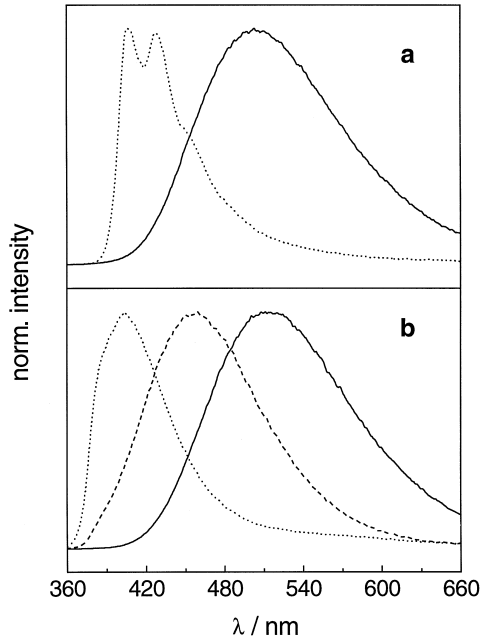

Fig. 1. (a) Fluorescence spectra of **1e34** (solid line) and **2e34** (dotted). (b) Fluorescence spectra of **1e23** (dashed), **1e4** (dotted) and **1e24** (solid). Solvent: acetonitrile.

the LE state (equilibrium) or charge recombination (i.e. recovery of the ground state).

In contrast, the emission of **1e34** is unstructured and shifted to the red, indicating a substantial dipole moment of the excited state. The lack of LE-type emission indicates highly efficient CT.

3.1.2. Computational

3.1.2.1. Geometry of the intramolecular CT state. In principle, one could optimize the geometry of the CT state and calculate the excitation energies using advanced ab initio methods like multiconfiguration SCF, e.g. CASSCF (complete active space self-consistent field) in combination with multireference second-order perturbation theory (CASPT2) [18]. However, in practice these methods can only be applied to systems of much smaller size. Therefore, we have to make some simplifying assumption concerning the geometry of the intramolecular CT state.

Biaromatic systems, consisting of a donor and an acceptor directly connected by a single σ-bond can undergo fast solvent-assisted relaxation from a primary excited singlet state to polar ICT state [10]. These processes are often discussed in terms of the TICT (twisted intramolecular charge transfer) state model [19,20]. Here, the torsional motion around the connecting σ-bond is assumed to be the relevant reaction coordinate for the charge separation step. In the TICT state both aromatic sub-π-systems are decoupled. The electronic DA interaction (which is necessary for a radiative decay of the TICT state) is provided by fluctuations of the twist angle around 90° [21]. On the basis of the TICT model the compounds presented here provide a 'double TICT problem since' since there are *three* aromatic subsystems connected via *two* single σ-bonds [1]. Simple consideration imposes both dihedral angles to be 90° to stabilize a maximum dipole moment (complete decoupling). However, our CNDO/S-CI calculation reveal a strong decrease of the dipole moment for ϑ_2, going towards 90°. The reason becomes evident

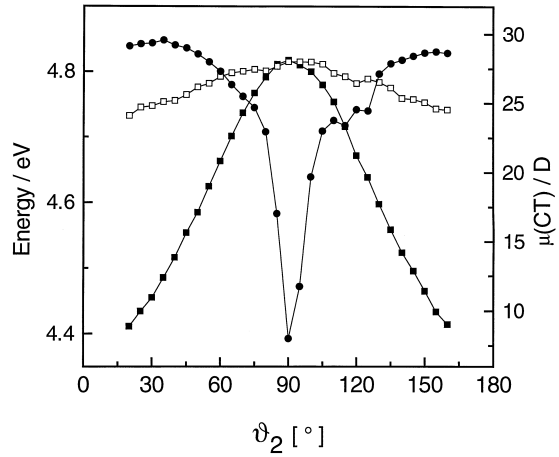

Fig. 2. Circles: calculated dipole moment of the lowest excited CT state in **1e34** using CNDO/S-CI; squares: calculated energies of the lowest (filled) and inverted CT (open). The quantities are calculated for various ϑ_2 values and a fixed $\vartheta_1 = 90°$ (for definition see text).

if one follows the energy of a second excited CT state (Fig. 2) in which charge is transferred from HOMO(A) (acceptors HOMO) into LUMO(D) (donors, LUMO). This *inverted* CT state has almost the same absolute dipole moment, but with opposite direction. The mixing of both states at ϑ_2 close to 90° due to pseudo degeneracy leads effectively to a compensation of dipole moments.

Furthermore, Fig. 2 shows that the energy of the CT state is minimal for small ϑ_2. Since similar mixings have been observed for all of these compounds, all calculations concerning the CT state are based on a perpendicular geometry with $\vartheta_1 = 90$ and $\vartheta_2 = 40°$.

Table 1
Calculated energies of the CT states, excitation energies for the orbital transition HOMO(D) → LUMO(A), differences in the corresponding orbital energies, and the values of the two-electron Coulomb integrals

	1e34	**2e34**	**1e23**	**1e24**	**1e4**
E(CT)	4.55	4.98	4.64	4.53	4.60
$\Delta E_{d \to a}$	4.91	5.20	5.19	4.86	4.98
$\epsilon_a - \epsilon_d$	6.43	6.60	6.55	6.38	6.54
(dd|aa)	1.52	1.40	1.36	1.52	1.56

d and a are abbreviations for HOMO(D) and LUMO(A), respectively. Calculations are based on a perpendicular geometry with $\vartheta_1 = 90°$ and $\vartheta_2 = 40°$ (see text). All quantities are in eV.

[1] The dihedral angle between pyrene and the phenyl ring in the center is described as ϑ_1. Correspondingly, the dihedral angle between the phenyl and the ester aromatic compound is decribed as ϑ_2.

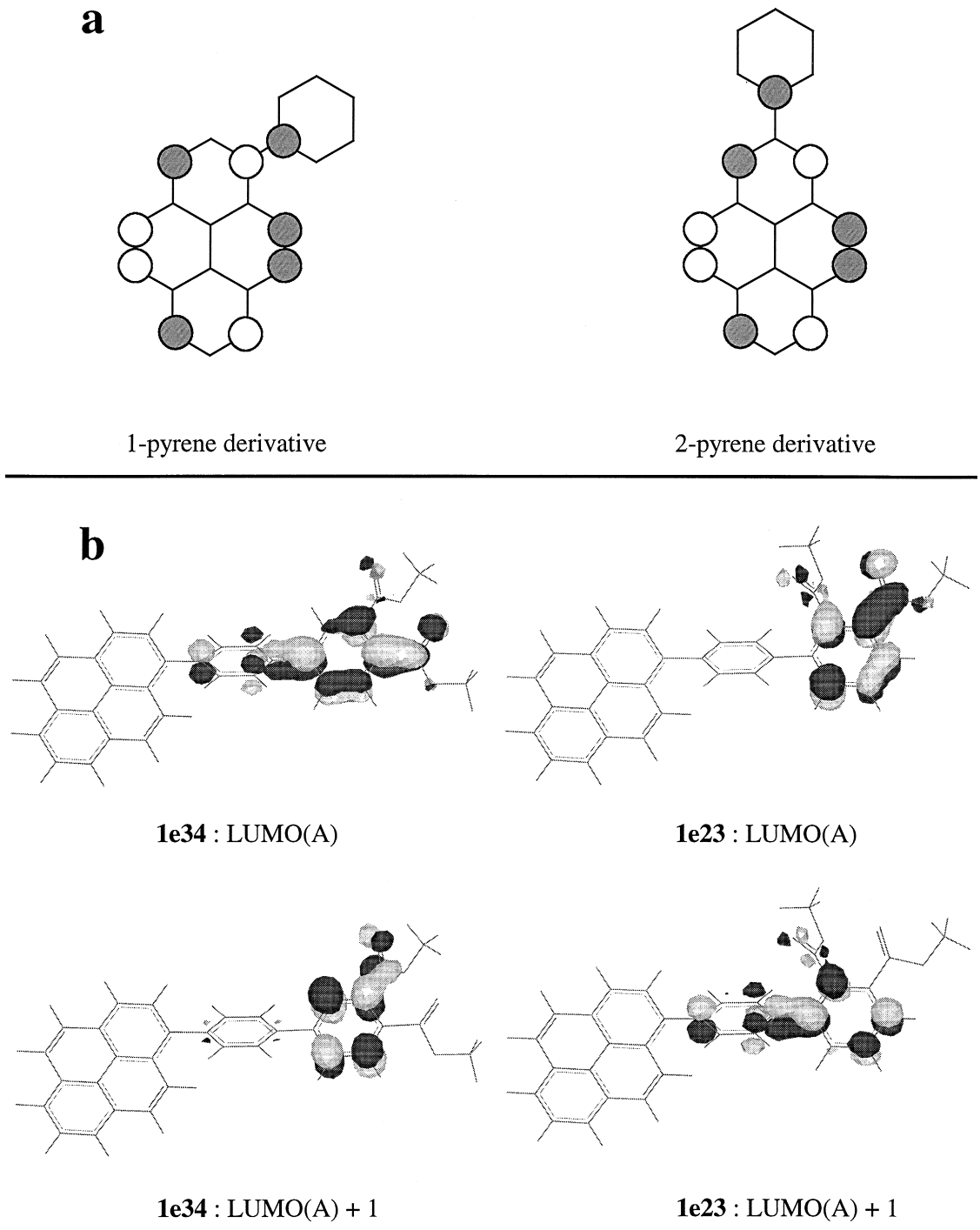

Fig. 3. (a) Schematic respresentation of the pyrene HOMO in the presence of an aromatic substituent in 1- and 2-position. (b) Acceptor molecular orbitals of **1e34** and **1e23** at perpendicular geometries ($\vartheta_1 = 90°$ and $\vartheta_2 = 40°$).

According to quantum chemical calculations (Table 1) the CT state of **2e34** is significantly higher in energy compared to that of **1e34**. This can be rationalized by regarding the nodal structure of the HOMO localized on the pyrene site (Fig. 3a). The 1-position shows a large MO coefficient in contrast to the 2-position. Consequently, intrinsic Coulomb interactions arise between the pyrene moiety and an aromatic substituent depending on the position of linkage.

The HOMO energy is increased when pyrene is substituted in 1-position whereas a substituent in 2-position has a much weaker influence to the HOMO energy. The higher the HOMO(D) energy the smaller the gap to the LUMO(A) localized on the ester site, i.e. the lower the energy for the CT orbital transition $\Delta E_{d\to a}$.

A second Coulomb effect results from the electronic repulsion due to the one-electron excitation. Its influence to the orbital transition energy $\Delta E_{d\to a}$ is represented by the two-center–two-electron Coulomb integral (dd|aa):

$$\Delta E_{d\to a} = \epsilon_a - \epsilon_d - (dd|aa) + 2(da|da), \qquad (1)$$

where ϵ_a and ϵ_d are the energies of the initial (donor) and the final (acceptor) orbital state, respectively, and (da|da) is a two-electron exchange integral that can mostly be neglected for CT transitions. A similar effect has already been described for rigidly linked aniline–naphthalene derivatives [22].

According to our calculations both effects contribute to the actual difference in CT state energies between **1e34** and **2e34**. Apparently, the CT state in **1e34** is stabilized due to favorable electronic interactions between the decisive donor and acceptor orbitals. This stabilization is missing in **2e34**, leading to a CT state significantly higher in energy.

This explanation is supported by the fact that the fluorescence of **2e34** decays single exponentially (75 ns) and independently of the detection wavelength. This fact is consistent with the following kinetic model: the LE and CT states are connected via an equilibrium which is fast compared to the deactivation of both of each state. However, since the CT formation is endothermic the equilibrium is strongly centered on the LE site. Consequently, the fluorescence decays single exponentially with a lifetime being determined by the radiative (and nonradiative) decay channels of the LE and CT states (in absence of the equilibrium!).

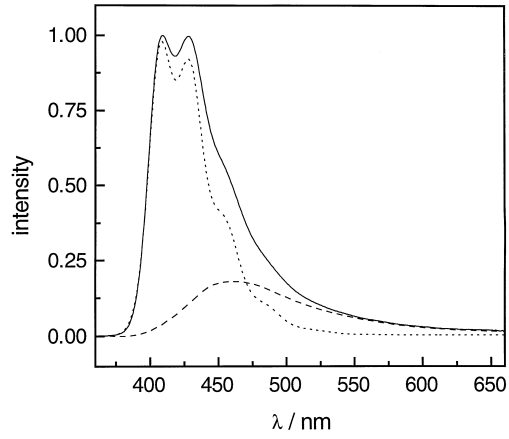

Fig. 4. Fluorescence spectra of **2e34** in acetonitrile (solid line). To separate the CT band (dashed line) the fluorescence spectrum of **2e34** in a non-polar solvent (cyclopentane, dotted) has been subtracted.

Additional support can be obtained by reconstructing the measured fluorescence spectrum of **2e34**. Therefore, we subtracted the fluorescence spectrum of **2e34** obtained in a non-polar solvent (cyclopentane) from the one recorded in acetonitrile. The result is shown in Fig. 4. The reconstructed maximum of the CT band is located at 460 nm, i.e. a hypsochromic shift of 40 nm compared to **1e34** corresponding to $\sim 2200\ cm^{-1}$. If one assumes similar repulsive Franck–Condon ground states in both systems one obtains an energy gap of ~ 0.3 eV between both CT states. This figure is in excellent agreement with our calculated data which reveal ~ 0.4 eV (see Table 1).

3.2. Influence of acceptor substitution

3.2.1. Experimental

Fig. 1b shows the fluorescence spectra of three different systems in which pyrene is substituted in the 1-position. The spectrum of **1e23** is similar to that of **2e34** (Fig. 1a). It shows a strong LE band near 400 nm and a significantly smaller part of red-shifted CT emission at ~ 550 nm. However, if only one methyl ester group on the acceptor site is shifted (see **1e24**, from meta to para) the fluores-

cence spectrum changes completely and becomes very similar to that obtained for **1e34**.

To clarify the important question whether differences in the acceptor strengths (i.e. reduction potentials) could be responsible for the different fluorescence properties of **1e23** and **1e34** we synthesized compound **1e4**. This system contains a benzoic acid ester fragment as electron acceptor which has significant weaker acceptor properties compared to the diester fragments in **1e23**, **1e24** and **1e34** [23]. As a consequence, the Stokes shift in the CT fluorescence is smaller compared to **1e34** or **1e24**. However, there can be no doubt that the CT efficiency is still very high in this system.

Differences in ΔG^{o} values (according to different reduction potentials of the acceptor) are apparently not responsible for the huge differences in the fluorescence spectra of **1e23** compared to **1e24** or **1e34**. Obviously, the molecular structure of the acceptor itself has a strong influence on the quantum yield of CT emission.

3.2.2. Computational

From CNDO/S-CI calculation one obtains a value for the lowest excited CT state in **1e23** which is slightly higher than for all other 1-pyrene derivatives (see Table 1), but still comparable to them regarding the estimated accuracy of the method (~ 0.1 eV). In contrast, the orbital transition energy for HOMO(D) $\rightarrow$ (LUMO(A) is noticeably large. Comparing the corresponding energy difference of the molecular orbitals one recognizes the Coulomb integral to be mainly responsible for the large CT orbital transition energy. The reason becomes evident if one regards the actual shape of the LUMO(A) orbitals, shown in Fig. 3b. The LUMO(A) of **1e23** is strongly localized on the outer aromatic system. It does not interact with the phenyl ring in the center due to the vanishing MO coefficient at the connecting carbon atom. As discussed above, this leads to a small Coulomb stabilization and consequently to a much higher value for the CT orbital transition energy.

Likewise, the electronic interaction with the pyrene moiety is weak, i.e. no sufficient electronic coupling is provided. However, the next higher acceptor MO of **1e23** (LUMO(A) + 1) is completely delocalized over the phenyl bridge. Consequently, for the Coulomb integral of the transition HOMO(D) $\rightarrow$ LUMO(A) + 1 one obtains a large value of 1.60 eV. The large Coulomb stabilization is actually responsible for the fact that the transition HOMO(D) $\rightarrow$ LUMO(A) + 1 has even a lower energy than the usual CT transition HOMO(D) $\rightarrow$ LUMO(A).

According to the CI calculation, the lowest CT state of **1e23** is a linear combination of both orbital transitions. Since, the HOMO(D) $\rightarrow$ LUMO(A) transition does not contribute to the electronic coupling, the overall coupling elements $\langle \mathrm{CT}|H|\mathrm{S}_0\rangle$ and $\langle \mathrm{CT}|H|\mathrm{LE}\rangle$ should be smaller compared to **1e24**, **1e34** or **1e4**, where $\langle \mathrm{CT}|$ consists mainly of one MO transition which provides strong electronic coupling.

In recent years, orbital symmetry effects on optical and thermal electron transfer in rigidly linked DA C_s-symmetric compounds have been reported [24,25]. However, those effects, which have been explained on the basis of symmetry requirements for $\langle \mathrm{CT}|H|\mathrm{S}_0\rangle$ are not directly related to the systems presented in this study.

3.3. Simulation of absorption spectra

Electronic transitions and their oscillator strengths have also been calculated to simulate the absorption spectra of these compounds. Fig. 5 shows the measured spectra together with the calculated results for two compounds **1e23** and **1e34** using the CNDO/S-CI method. These compounds have been selected because of their pronounced differences in the region between 280 and 300 nm. Furthermore, **1e34** show a red-shifted tailing between 350 and 400 nm.

The spectra are characterized by the typical vibrational structure of pyrene in solution which is, however, strongly washed-out in these compounds. Particularly, the red edges of the spectra are broadened and Stokes shifted which might be due to vibronic interaction between the S_1 and the S_2 state of pyrene [27]. In fact, CNDO/S-CI calculations indicate a smaller S_1–S_2 energy gap for 1-phenyl pyrene than for pyrene itself, which supports this interpretation.

Fig. 5 shows also satisfactory agreement between calculated data and the measured spectra. It is interesting to note, that **1e34** — a compound with high CT efficiency — show also a larger Stokes shift in the $S_2 \leftarrow S_0$ absorption band which is nicely reproduced by the simulation.

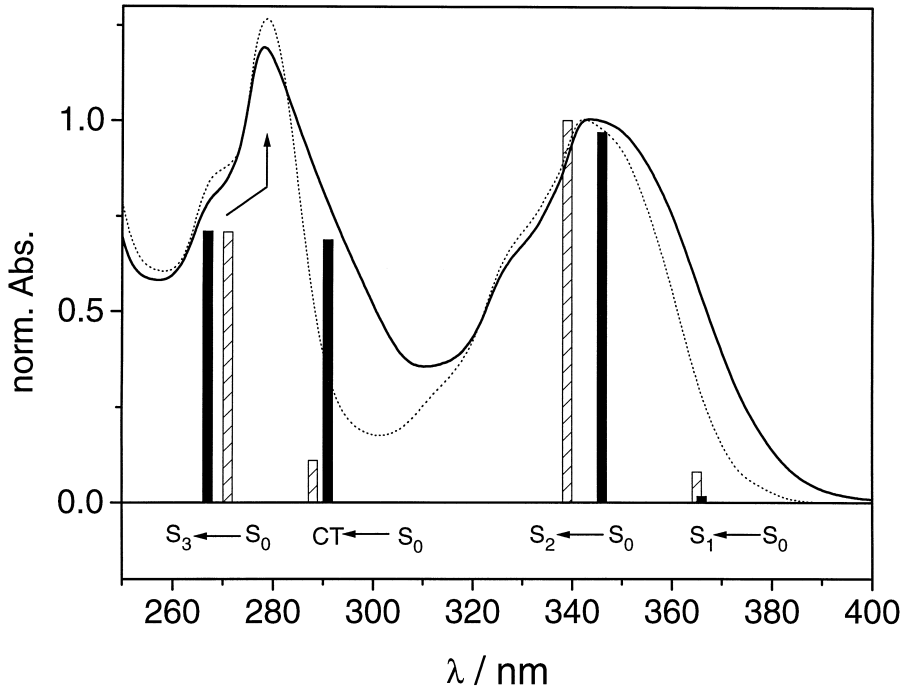

Fig. 5. Normalized UV absorption spectra of **1e34** (solid line) and **1e23** (dotted line) in acetonitrile. The bars represent the vertical excitation energies and the corresponding (normalized) oscillator strengths as obtained from CNDO/S-CI calculations. The nomenclature of the S_n states is refered to the unsubstituted pyrene [26].

Furthermore, the calculation indicates the existence of an optical CT (OCT) absorption band between 280 and 300 nm. According to simple perturbation theory approaches for OCT [28] the extinction is proportional to the electronic coupling matrix element between the ground and the CT state. This leads to a consistency between fluorescence and absorption data and supports our interpretation that the significantly reduced electronic coupling between donor and acceptor is responsible for the lack of CT emission in **1e23**.

4. Conclusions

In this Letter we present experimental and theoretical studies on a series of compounds to address the effect of structural variations on CT efficiencies in extended donor–acceptor π-systems. Slight changes in the substitution scheme of intramolecular DA systems can lead to completely different spectroscopic properties. This might be either due to differences in the electronic coupling between the DA moieties or due to energy changes of specific excited states. By applying semiempirical quantum chemical calculations one can gain qualitative information about the magnitude of electronic coupling and the relative energy of CT states. Therefore, these calculations might be valuable implications for the design of high-efficient CT dyes.

Our experimental and theoretical results show that charge transfer in conjugated systems cannot be treated in terms of simple electron transfer theories which are mainly based on thermodynamic arguments [14]. The difference in redox potentials of donor and acceptor does influence the spectral position of a CT emission band; however, the nature of the emitting species in general is strongly influenced by the electronic interactions between particular molecular orbitals. The shape of these orbitals is mostly predictable using simple molecular orbital theory.

Preliminary femtosecond time-resolved measurements on these compounds have been carried out

[29]. We hope to be able to relate these data to our studies presented in this Letter.

Acknowledgements

We warmly thank Professor Sven Larsson and Professor Ahmed Zewail (Caltech) for various fruitful discussions. Additionally we are very grateful to Sven Larsson for providing the CNDO/S code. J. Schimpfhauser, J. Bienert, H. Meyer and B. Frederichs have supported this work by technical assistance. TF is grateful to the Fonds der Chemischen Industrie for financial support.

References

[1] J.R. Bolton, J.A. Schmidt, T.F. Ho, Adv. Chem. Ser., Electron Transfer Inorg. Org. Biol. Syst. 228 (1991) 117–131.
[2] J. Rodriguez, C. Kirmaier, M.R. Johnson, R.A. Friesner, D. Holten, J.L. Sessler, J. Am. Chem. Soc. 113 (1991) 1652.
[3] D. Heiler, G. McLendon, P. Rogalskyj, J. Am. Chem. Soc. 109 (1987) 604.
[4] A. Wiessner, G. Hüttmann, W. Kühnle, H. Staerk, J. Phys. Chem. 99 (1995) 14923.
[5] K. Tominaga, G.C. Walker, W. Jarzeba, P.F. Barbara, J. Phys. Chem. 95 (1991) 10475.
[6] J. Herbich, J. Waluk, Chem. Phys. 188 (1994) 247.
[7] H. Port, G. Quapil, H.C. Wolf, F. Effenberger, C.-P., Niesert, R. Buhleier, Z. Gogolak, J. Kuhl, in: G.A. Mourou, A.H. Zewail (Eds.), Ultrafast Phenomena VIII, Springer Series, Springer, Berlin, 1992, p.596.
[8] A. Onkelix, F.C. De Schryver, L. Vieane, M. Van der Auweraer, K. Iwai, M. Yamamoto, M. Ichikawa, H. Masahura, M. Maus, W. Rettig, J. Am. Chem. Soc. 118 (1996) 2892.
[9] M. Braga, S. Larsson, Chem. Phys. Lett. 213 (1993) 217.
[10] W. Rettig, M. Maus, R. Lapouyade, Ber. Bunsenges., Phys. Chem. 100 (1996) 2091.
[11] J. Hopfield, Proc. Natl. Acad. Sci. USA 71 (1974) 3640.
[12] J. Jortner, J. Chem. Phys. 64 (1976) 4860.
[13] R.A. Marcus, J. Chem. Phys. 81 (1984) 4494.
[14] A. Weller, Z. Phys. Chem. 133 (1982) 93.
[15] J. Del Bene, H.H. Jaffé, J. Chem. Phys. 48 (1968) 1807.
[16] J. Del Bene, H.H. Jaffé, J. Chem. Phys. 49 (1968) 1221.
[17] MOPAC 6.0: QCPE program #455.
[18] B.O. Roos, M.P. Fulscher, P.A. Malmquist, M. Merchan, L. Serrano-Andres, in: S.R. Langhoff (Ed.), Quantum Mechanical Electronic Structure Calculations with Chemical Accuracy, Kluwer, Dordrecht, 1994.
[19] K. Rotkievicz, Z.R. Grabowski, K.H. Grellmann, Chem. Phys. Lett. 19 (1973) 315.
[20] T. Okada, T. Fujita, M. Kubota, S. Masaki, N. Mataga, R. Ide, Y. Sakata, S. Misumi, Chem. Phys. Lett. 14 (1972) 563.
[21] M. van der Auweraer, Z.R. Grabowski, W. Rettig, J. Phys. Chem. 94 (1990) 1443.
[22] W. Rettig, R. Haag, J. Wirz, Chem. Phys. Lett. 180 (1991) 216.
[23] L. Meites, P. Zuman, Electrochemical Data, part I, vol. A, Wiley, New York, 1974.
[24] Y. Zeng, M.B. Zimmt, J. Phys. Chem. 96 (1992) 8395.
[25] A.M. Oliver, M.N. Paddon-Row, J. Kroon, J.W. Verhoeven, Chem. Phys. Lett. 191 (1992) 371.
[26] J.B. Birks, Photophysics of Aromatic Molecules, Wiley-Interscience, New York, 1970, p.71.
[27] G. Marconi, P.R. Salvi, Chem. Phys. Lett. 123 (1986) 254.
[28] N.S. Hush, Electrochim. Acta 13 (1968) 1005.
[29] T. Fiebig, M. Chachisvilis, A.H. Zewail (work in progress at Calif. Inst. Technol., Pasadena, CA).